UKACC International Conference on Control 2012
Cardiff, UK, 3-5 September 2012

Singular Perturbation Control of the Longitudinal Flight Dynamics of an UAV

Sergio Esteban
Department of Aerospace Engineering
University of Seville
Seville, Spain 41092
Email: sesteban@.us.es

Damián Rivas
Department of Aerospace Engineering
University of Seville
Seville, Spain 41092
Email: drivas@.us.es

***Abstract*—This paper presents a singular perturbation control strategy for regulating the longitudinal flight dynamics of an Unmanned Air Vehicle (UAV). The proposed control strategy is based on a four-time-scale (4TS) decomposition that includes the altitude, velocity, pitch, and flight path angle dynamics, with the control signals being the elevator deflection and the throttle position. The nonlinear control strategy drives the system to follow references in the aerodynamic velocity and the flight path angle. In addition, the control strategy permits to select the desired dynamics for all the singularly perturbed subsystems. Numerical results are included for a realistic nonlinear UAV model, including saturation of the control signals.**

I. Introduction

Historically, classical linear control techniques have been sufficient to obtain reasonable control responses of aerospace systems, but the evolution of the aerospace industry, and the consequent improvement of technologies, have increased the performance requirements of all systems in general, which has called for better control designs that can deal with more complex systems. Specifically, in the area of aerospace systems, a wide range of different nonlinear control techniques have been studied to deal with the nonlinear dynamics of such systems. From singular perturbation [1], [2], feedback linearization [3], dynamic inversion [4], sliding mode control [5], or backstepping control methods [6], [7], to name a few. Neural Networks (NN) are also included within the realm of nonlinear control techniques, and seem to provide improved robustness properties under system uncertainties. Some of works include Adaptive Critic Neural Network (ACNN) based controls, originally presented by Balakrishnan and Biega [8], and later extended to many other aerospace systems [9].

One of the most challenging tasks in control is the modeling of systems in which the presence of parasitic parameters, such as small time constants, is often the source of a increased order and stiffness [10]. The stiffness, attributed to the simultaneous occurrence of slow and fast phenomena, gives rise to time-scales, and the suppression of the small parasitic variables results in degenerated, reduced-order systems called singularly perturbed systems (SPS), that can be stabilized separately, thus simplifying the burden of control design of high-order systems.

The application of singular perturbation and time-scale techniques in the aerospace industry can be traced back to the 1960s when it was first applied to solve complex flight optimization problems [11]. Since then, singular perturbation and time-scale techniques have been extensively used in the aerospace industry as described in the extense literature review conducted by Naidu and Calise [10]. In recent years these techniques have been also extended to UAVs [2], [12].

The objective of this paper is to develop a singular perturbation control strategy for the longitudinal dynamics of an aircraft, that be able to follow references in aerodynamic velocity and flight path angle, using as control actuators the elevator deflection and the throttle position. In addition, the proposed singular perturbation control strategy permits to select the desired closed-loop dynamics of each of the resulting reduced-order and boundary-layer subsystems using a time-scale analysis similar to those presented in [2], [13]. Simulations are included for a realistic UAV model including nonlinear dynamics and actuator saturation on both the elevator deflection and throttle setting. The model used corresponds to the Cefiro aircraft [14], an UAV recently designed and constructed by the authors at the University of Seville.

This paper is structured as follows: Section II presents the flight dynamics used throughout this work; Section III presents the time scales selection; Section IV describes the proposed 4-time-scale analysis; the singular perturbed control strategies are presented in Section V; numerical results for the UAV model considered in this paper are given in Section VI; and finally, some conclusions are drawn in Section VII.

II. Model Definition

The problem discussed in this article considers a constant-mass UAV with an electrical propulsion plant, for which the point-mass longitudinal flight dynamics equations are

$$\dot{h} = V \sin\gamma, \tag{1}$$

$$\dot{V} = \frac{1}{m}\left(T - D - mg\sin\gamma\right), \tag{2}$$

$$\dot{\theta} = q, \tag{3}$$

$$\dot{\gamma} = \frac{1}{mV}\left(L - mg\cos\gamma\right). \tag{4}$$

$$\dot{q} = \frac{M}{I_y}, \tag{5}$$

where h is the altitude; V the aerodynamic speed; γ the flight path angle; θ the pitch angle; q the pitch rate; T, D, and L the thrust, drag, and lift forces, respectively; M the total pitch

moment; m and I_y the mass and the moment of inertia of the UAV. The thrust-force model used is given by

$$T = \delta_T(T_0 + T_1 V + T_2 V^2), \tag{6}$$

where δ_T is the throttle setting, $0 \leq \delta_T \leq 1$ and T_0, T_1, T_2 are known coefficients obtained through wind tunnel experiments. The lift, drag and pitch moment are given by the following expressions

$$L = q_\infty S C_L,\ D = q_\infty S C_D,\ M = q_\infty S c C_M, \tag{7}$$

where $q_\infty = 1/2\rho V^2$ is the dynamic pressure; S is the reference wing area, c is the wing mean aerodynamic chord, and C_L, C_D and C_M are the lift, drag and pitch moment coefficients, which are given by the following standard models [15], [16] that have been widely used in the literature [11], [17], [18]

$$C_L = C_{L_0} + C_{L_\alpha}\alpha + C_{L_\delta}\delta, \tag{8}$$
$$C_D = C_{D_0} + kC_L^2, \tag{9}$$
$$C_M = C_{M_0} + C_{M_\alpha}\alpha + C_{M_\delta}\delta + C_{M_q}q, \tag{10}$$

where α is the angle of attack, given by $\alpha = \theta - \gamma$, δ is the elevator deflection, $-40^\circ \leq \delta \leq 40^\circ$, and C_{L_0}, C_{L_α}, C_{L_δ}, C_{D_0}, k, C_{M_0}, C_{M_α}, C_{M_δ}, and C_{M_q} are known aerodynamic coefficients. In this paper the simplifying assumption of constant air density is considered, and, therefore, the altitude equation becomes decoupled from the rest, and can be solved a posteriori. Equations (1–5) are expanded using Eqns. (8–10), resulting in

$$\dot{h} = V\sin\gamma, \tag{11}$$
$$\dot{V} = \delta_T(a_1 + a_2V^2 + a_3V) + V^2\left[a_4 + a_5 + a_6\left(\theta-\gamma\right) + a_7\left(\theta-\gamma\right)^2 + a_8\delta + a_9\delta^2 + a_{10}\left(\theta-\gamma\right)\delta\right] + a_{11}\sin\gamma, \tag{12}$$
$$\dot{\theta} = q, \tag{13}$$
$$\dot{\gamma} = V\left[a_{12} + a_{13}\left(\theta-\gamma\right) + a_{14}\delta\right] + \frac{a_{11}}{V}\cos\gamma, \tag{14}$$
$$\dot{q} = V^2\left[a_{15} + a_{16}\left(\theta-\gamma\right) + a_{17}\delta + a_{18}q\right], \tag{15}$$

where $a_1 = T_0/m$, $a_2 = T_2/m$, $a_3 = T_1/m$, $a_4 = -c_2C_{D_0}$, $a_5 = -c_1C_{L_0}^2$, $a_6 = -2c_1C_{L_0}C_{L_\alpha}$, $a_7 = -c_1C_{L_\alpha}^2$, $a_8 = -2c_1C_{L_0}C_{L_\delta}$, $a_9 = -c_1C_{L_\delta}^2$, $a_{10} = -2c_1C_{L_\alpha}C_{L_\delta}$, $a_{11} = -g$, $a_{12} = c_2C_{L_0}$, $a_{13} = c_2C_{L_\alpha}$, $a_{14} = c_2C_{L_\delta}$, $a_{15} = c_3C_{M_0}$, $a_{16} = c_3C_{M_\alpha}$, $a_{17} = c_3C_{M_\delta}$, $a_{18} = c_3C_{M_q}$ with $c_1 = \rho Sk/(2m)$, $c_2 = \rho S/(2m)$, and $c_3 = \rho Sc/(2I_y)$.

The underactuated structure of the system requires that two variables need to be used as references. In this work, the nonlinear control strategy will seek to drive the system to follow references in the aerodynamic velocity and the flight path angle, that is $V = V_{ref}$ and $\gamma = \gamma_{ref}$.

III. TIME SCALES SELECTION

The appropriate selection of time scales is an important aspect of the singular perturbation and time-scales theory [10], [19]–[21], and can be categorized into three approaches: 1) direct identification of small parameters (such as small time constants); 2) transformation of state equations; and 3) linearization of the state equations. Ardema [19] proposes a rational method of identifying time scales separations that does not rely on an *ad hoc* selection of time scales based largely on physical insight and past experiences with similar problems. The proposed method only requires a knowledge of the state equations. Considering a dynamical systems of the form

$$\dot{x} = f(x,u),\ u \in U, \tag{16}$$

subject to suitable boundary conditions, where x is an n-dimensional state vector, u an r-dimensional control vector, and U the set of admissible controls. It is assumed that bounds have been established on the components of the state vector, either by physical limitations or by a desire to restrict the state to a certain region of state space, $x_{i,m} \leq x_i \leq x_{i,M}$, with $x_{i,m}$ and $x_{i,M}$ representing the minimum and maximum values of the state variables. As noted in [19], most *ad hoc* assessments of time-scale separation are based on the concept of state variable speed [11], [22]. The speed of a state variable x_i is defined as the inverse of the time it takes that variable to change across a specified range of values, which can be expressed as

$$S_i = \frac{\dot{x_i}}{\Delta x_i} = \frac{f_i(x,u)}{\Delta x_i}. \tag{17}$$

where $\Delta x_i = x_{i,M} - x_{i,m}$. Two methods are proposed [19] to determine if two variables are candidates for time-scale separation, which is ultimately defined if the two variables have widely separated speeds. In this work, the method that considers a reference value of the state in the region of interest, $\bar{x}$, is adopted, hence

$$S_i = \frac{1}{\Delta x_i}\max_{u\in U} f_i(\bar{x},u). \tag{18}$$

Since the maneuvers being considered for the UAV are those of climb performance, the reference states can be selected as those associated to the condition of maximum rate of climb $V_{v_{max}}$, condition that has been investigated in [14]. The bounds for the UAV model considered in this article [14] are therefore: $0 \leq h \leq 1000$, where the maximum altitude is defined by desired operation limits; $V_m \leq V \leq V_{max}$, with $V_m = 1.2 * V_{stall}$, and V_{max} obtained in the performance analysis [14]; $-\gamma_{d_{max}} \leq \gamma \leq \gamma_{V_m}$, where $\gamma_{d_{max}}$ represents the maximum descent glide angle, and γ_{V_m} represents the maximum flight path angle at V_m; $\alpha_{trim_{V_m}} \leq \alpha \leq \alpha_{trim_{V_{max}}}$, where $\alpha_{trim_{V_m}}$ and $\alpha_{trim_{V_{max}}}$ corresponds to the trim angle for V_m, and V_{max}, respectively; $\theta_m \leq \theta \leq \theta_M$ with $\theta_m = \gamma_m + \alpha_m$ and $\theta_M = \gamma_M + \alpha_M$; and finally, the bounds for the pitch rate $q_m \leq q \leq q_M$ are selected by desired operation limits.

From [14], the UAV being studied in this article has the following geometric properties, $S = 1.088\ m^2$, $c = 0.393\ m$, $m = 23.186\ kg$, $I_y = 7.447\ kgm^2$, $C_{D_0} = 0.0286$, $k = 0.0426$. From the stability analysis conducted in [14], the derivatives are: $C_{L_0} = 0.408$, $C_{M_0} = 0.0617$, $C_{L_\alpha} = 3.823$ per rad, $C_{M_\alpha} = -0.455$ per rad, $C_{L_\delta} = 0.284$ per rad, $C_{M_\delta} = -0.914$ per rad, $C_{M_q} = -13.590$ s/rad, $T_0 = 127.53N$, $T_1 = -2.9052 \times 10^{-1} Ns/m$ and $T_2 = -5.9616 \times 10^{-2} Ns^2/m^2$.

From the performance study in [14], it can be obtained that the maximum vertical climb speed is $V_{v_{max}} = 27.00$ m/s, the reference horizontal speed is $\bar{V} = 22.90\ m/s$, the stall velocity is given by $V_{stall} = 14.38\ m/s$, for $C_{L_{max}} = 1.65$, the maximum velocity $V_{max} = 38.47\ m/s$, the flight path angle for $\bar{V}$ is given $\gamma_{\bar{V}} = 19.06^\circ$, the gliding angle for minimum flight path angle is given by $\gamma_{V_d} = -7.63^\circ$, the trim

angles for $\bar{V}$ are given by $\alpha_{trim_{\bar{V}}} = 3.47^\circ$ and $\delta_{trim_{\bar{V}}} = 2.14^\circ$ respectively. The final bounds and *speeds* of the state variables are resumed in Table I. It can be seen four clearly differentiated time-scales, since the *speeds* for altitude and velocity dynamics are not that separated, therefore, it will be assumed that they move in the same stretched time scale, and will be denoted by the augmented state vector $\chi = [h\ V]$.

TABLE I
BOUNDS AND *speeds* OF THE STATE VARIABLES.

Variable	$x_{i,m}$	$x_{i,M}$	Δx_i	$\bar{x}_i$	S_i
h [m]	0	1000	1000	200	0.0074
V [m/s]	17.25	38.47	21.21	22.90	0.011
θ [deg]	-7.58	32.84	40.42	22.53	0.41
γ [deg]	-4.53	23.31	27.83	19.06	2.21
α [deg]	-3.06	9.53	12.59	3.47	N/A
q [deg/s]	-264.44	264.44	528.88	0	82.43

With this in mind, Eqns. (11–15) are rewritten as a four-time-scale (4TS) singular perturbed model of the form

$$\dot{\chi} = f_\chi(\chi, \theta, \gamma, \delta, \delta_T),\ \chi \in B_\chi, \tag{19}$$
$$\varepsilon_1 \dot{\theta} = f_\theta(q),\ \theta \in B_\theta, \tag{20}$$
$$\varepsilon_1\varepsilon_2 \dot{\gamma} = f_\gamma(\chi, \theta, \gamma, \delta),\ \gamma \in B_\gamma, \tag{21}$$
$$\varepsilon_1\varepsilon_2\varepsilon_3 \dot{q} = f_q(\chi, \theta, \gamma, q, \delta),\ q \in B_q, \tag{22}$$

with $B_\chi, B_\theta, B_\gamma, B_q$ denoting closed sets of the variables χ, θ, γ and q, respectively, being χ the slowest variable, θ the intermediate variable, γ the fast variable, and q the ultra-fast variable, and holding that $0 < \varepsilon_1\varepsilon_2\varepsilon_3 \ll \varepsilon_1\varepsilon_2 \ll \varepsilon_1 \ll 1$. In order to express the original set of differential Eqns. (11–15) in the standard 4TS singular perturbation formulation, a series of algebraic modifications using the *speeds* of the different variables are conducted. Let consider the different *speeds* as if they were the inverse of the inertias multiplying the time derivatives such $I_h = 1/S_h = 133.722$, $I_V = 1/S_V = 89.221$, $I_\theta = 1/S_\theta = 2.411$, $I_\gamma = 1/S_\gamma = 0.451$, $I_q = 1/S_q = 0.012$, where it can be easily identified that $I_V >> I_\theta >> I_\gamma >> I_q$, therefore, in order to express the equations of the 4TS in the correct multi-time singular perturbation formulation, all the perturbation parameters are normalized with respect to the slowest coefficient, that is I_h, yielding the parasitic constants selected for this problem given by $\varepsilon_1 = I_\theta/I_h = 1.803\times10^{-2}$, $\varepsilon_1\varepsilon_2 = I_\gamma/I_h = 3.375\times10^{-3}$, and $\varepsilon_1\varepsilon_2\varepsilon_3 = I_q/I_h = 9.0722\times10^{-5}$, resulting in

$$\dot{h} = V\sin\gamma, \tag{23}$$
$$\dot{V} = \delta_T\left(a_1 + a_2V^2 + a_3V\right) + V^2\left[a_4 + a_5 + a_6\left(\theta-\gamma\right)\right. + a_7\left(\theta-\gamma\right)^2 + a_8\delta + a_9\delta^2 + \left. a_{10}\left(\theta-\gamma\right)\delta\right] + a_{11}\sin\gamma, \tag{24}$$
$$\varepsilon_1\dot{\theta} = \varepsilon_1 q, \tag{25}$$
$$\varepsilon_1\varepsilon_2\dot{\gamma} = V\left[\bar{a}_{12} + \bar{a}_{13}\left(\theta-\gamma\right) + \bar{a}_{14}\delta\right] + \frac{\bar{a}_{11}}{V}\cos\gamma, \tag{26}$$
$$\varepsilon_1\varepsilon_2\varepsilon_3\dot{q} = V^2\left[\bar{a}_{15} + \bar{a}_{16}\left(\theta-\gamma\right) + \bar{a}_{17}\delta + \bar{a}_{18}q\right], \tag{27}$$

with $\bar{a}_{11} = \varepsilon_1\varepsilon_2 a_{11}$, $\bar{a}_{12} = \varepsilon_1\varepsilon_2 a_{12}$, $\bar{a}_{13} = \varepsilon_1\varepsilon_2 a_{13}$, $\bar{a}_{14} = \varepsilon_1\varepsilon_2 a_{14}$, $\bar{a}_{15} = \varepsilon_1\varepsilon_2\varepsilon_3 a_{15}$, $\bar{a}_{16} = \varepsilon_1\varepsilon_2\varepsilon_3 a_{16}$, $\bar{a}_{17} = \varepsilon_1\varepsilon_2\varepsilon_3 a_{17}$, and $\bar{a}_{18} = \varepsilon_1\varepsilon_2\varepsilon_3 a_{18}$. In addition, the following approximations are considered in this article (which have been widely used in the literature for aircraft trajectory optimization using singular perturbation techniques [11])

$$\sin\gamma \cong \gamma - \frac{\gamma^3}{6},\ \cos\gamma \cong 1 - \frac{\gamma^2}{2}, \tag{28}$$

The following section describes the four-time-scale analysis that will permit to derive the singular perturbation control strategy.

IV. 4-TIME-SCALE ANALYSIS

This section presents a sequential time-scale methodology that provides an approach in which, for a specific class of singularly perturbed nonlinear systems, a step-by-step procedure can be employed to design the proper control laws that guarantee a desired degree of stability of each of the time-scale subsystems. The approach is based on the sequential time-scale analysis similar to the one presented in [2], [13], which is an extension of the two-time-scale analysis presented in [1]. The approach consists in decomposing the original singularly perturbed system, Eqns. (23–27), denoted as Σ_{SIFU} for simplicity, into a sequential set of two-time-scale (2TS) SPS. Each one of the letters in Σ_{SIFU} denotes a time scale, Slow, Intermediate, Fast, and Ultrafast, and will be used as a reference to describe each time-scale subsystem or combination. The time-scale decomposition is achieved by applying, in a sequential manner, the associated stretched time scales for each of the subsystems, resulting in reduced order models. The time-scale decomposition is started by applying first the stretched time scale given by $\tau_3 = t/(\varepsilon_1\varepsilon_2\varepsilon_3)$, resulting in a 2TS SPS formed by the reduced order Σ_{SIF}-subsystem

$$\dot{h} = V\left(\gamma - \frac{\gamma^3}{6}\right), \tag{29}$$
$$\dot{V} = \delta_T\left(a_1 + a_2V^2 + a_3V\right) + V^2\left[a_4 + a_5 + a_6\left(\theta-\gamma\right)\right. + a_7\left(\theta-\gamma\right)^2 + a_8\delta + a_9\delta^2 + \left. a_{10}\left(\theta-\gamma\right)\delta\right] + a_{11}\left(\gamma - \frac{\gamma^3}{6}\right), \tag{30}$$
$$\varepsilon_1\dot{\theta} = \varepsilon_1 H_q(\theta, \gamma, \delta), \tag{31}$$
$$\varepsilon_1\varepsilon_2\dot{\gamma} = V\left[\bar{a}_{12} + \bar{a}_{13}\left(\theta-\gamma\right) + \bar{a}_{14}\delta\right] + \frac{\bar{a}_{11}}{V}\left(1 - \frac{\gamma^2}{2}\right), \tag{32}$$

and the boundary layer (fast), denoted as Σ_U-subsystem for simplicity, given by

$$\frac{dq}{d\tau_3} = V^2\left[\bar{a}_{15} + \bar{a}_{16}\left(\theta-\gamma\right) + \bar{a}_{17}\delta + \bar{a}_{18}q\right], \tag{33}$$

where $H_q(\theta, \gamma, \delta)$ represents the quasi-steady-state equilibrium (QSSE) of the boundary layer Σ_U-subsystem when setting $\varepsilon_3 = 0$, that is $0 = f_q(\chi, \theta, \gamma, q, \delta) \rightarrow \bar{q} = H_q(\theta, \gamma, \delta)$, resulting in

$$\bar{q} = H_q(\theta, \gamma, \delta) = -\frac{\bar{a}_{15} + \bar{a}_{16}(\theta-\gamma) + \bar{a}_{17}\delta}{\bar{a}_{18}}. \tag{34}$$

Recall that in the space of configuration of the boundary layer Σ_U-subsystem, the variables, χ, θ, and γ, are treated like fixed parameters. The time scale analysis continues recognizing that the reduced order Σ_{SIF}-subsystem, Eqns. (29–32), can be decomposed again into a 2TS SPS by applying the stretched time scale $\tau_2 = t/(\varepsilon_1\varepsilon_2)$, resulting in a new reduced order (slow) subsystem, denoted as Σ_{SI}-subsystem

for simplicity, defined as

$$\dot{h} = V\left(H_\gamma - \frac{H_\gamma^3}{6}\right), \tag{35}$$

$$\begin{aligned}\dot{V} &= \delta_T\left(a_1 + a_2V^2 + a_3V\right) + V^2\left[a_4 + a_5 + a_6\left(\theta - H_\gamma\right)\right.\\ &+ a_7\left(\theta - H_\gamma\right)^2 + a_8\delta + a_9\delta^2\\ &+ \left.a_{10}\left(\theta - H_\gamma\right)\delta\right] + a_{11}\left(H_\gamma - \frac{H_\gamma^3}{6}\right),\end{aligned} \tag{36}$$

$$\varepsilon_1\dot{\theta} = -\frac{\varepsilon_1\left(\bar{a}_{15} + \bar{a}_{16}(\theta - H_\gamma) + \bar{a}_{17}\delta\right)}{\bar{a}_{18}}, \tag{37}$$

and with a new boundary layer (fast) subsystem, denoted as Σ_F-subsystem for simplicity, given by

$$\frac{d\gamma}{d\tau_2} = V\left[\bar{a}_{12} + \bar{a}_{13}\left(\theta - \gamma\right) + \bar{a}_{14}\delta\right] + \frac{\bar{a}_{11}}{V}\left(1 - \frac{\gamma^2}{2}\right), \tag{38}$$

where $H_\gamma(\chi, \theta, \delta)$ represents the QSSE of the boundary layer Σ_F-subsystem when setting $\varepsilon_2 = 0$, that is $0 = f_\gamma(\chi, \theta, \gamma, \delta) \rightarrow \bar{\gamma} = H_\gamma(\chi, \theta, \delta)$, resulting in

$$\bar{\gamma} = H_\gamma(\chi, \theta, \delta) = A_1 \pm A_2\sqrt{A_3 + A_4\theta + A_5\delta}, \tag{39}$$

with $A_1 = -a_{13}V^2/a_{11}$, $A_2 = 1/a_{11}$, $A_3 = a_{13}^2V^4 + 2a_{11}a_{12}V^2 + 2a_{11}^2$, $A_4 = 2a_{11}a_{13}V^2$ and $A_5 = 2a_{11}a_{14}V^2$, where it can be shown that the positive solution is the valid one, and where χ, and θ are treated like fixed parameters. Finally, it can be recognized that the Σ_{SI}-subsystem can be decomposed one more time into another 2TS SPS by considering the last stretched time scale $\tau_1 = t/\varepsilon_1$, resulting in a new reduced order (slow) subsystem, denoted as Σ_S-subsystem for simplicity, and given by

$$\dot{h} = V\left(\bar{H}_\gamma - \frac{\bar{H}_\gamma^3}{6}\right), \tag{40}$$

$$\begin{aligned}\dot{V} &= \delta_T\left(a_1 + a_2V^2 + a_3V\right) + V^2\left[a_4 + a_5 + a_6\left(H_\theta - \bar{H}_\gamma\right)\right.\\ &+ a_7\left(H_\theta - \bar{H}_\gamma\right)^2 + a_8\delta + a_9\delta^2\\ &+ \left.a_{10}\left(H_\theta - \bar{H}_\gamma\right)\delta\right] + a_{11}\left(\bar{H}_\gamma - \frac{\bar{H}_\gamma^3}{6}\right),\end{aligned} \tag{41}$$

with the boundary layer Σ_I-subsystem given by

$$\frac{\mathrm{d}\theta}{\mathrm{d}\tau_1} = -\frac{\varepsilon_1\left(\bar{a}_{15} + \bar{a}_{16}(\theta - H_\gamma) + \bar{a}_{17}\delta\right)}{\bar{a}_{18}}, \tag{42}$$

where $H_\theta(\chi, \delta)$ represents the QSSE of the boundary layer Σ_I-subsystem when setting $\varepsilon_1 = 0$, that is $0 = f_\theta(\chi, \theta, \delta) \rightarrow \bar{\theta} = H_\theta(\chi, \delta)$, resulting in

$$H_\theta(\chi, \delta) = A_6 \pm A_7\sqrt{A_8 + A_9\delta} + A_{10}\delta, \tag{43}$$

with $A_6 = A_2^2A_4/2 - \bar{a}_{15}/\bar{a}_{16} + A_1$, $A_7 = A_2/(2\bar{a}_{16})$, $A_8 = \bar{a}_{16}^2A_2^2A_4^2 - 4\bar{a}_{15}\bar{a}_{16}A_4 + 4\bar{a}_{16}^2A_3 + 4\bar{a}_{16}^2A_1A_4$, $A_9 = 4\bar{a}_{16}^2A_5 - 4\bar{a}_{16}\bar{a}_{17}A_4$, and $A_{10} = \bar{a}_{17}/\bar{a}_{16}$. Recall also that $\bar{H}_\gamma(\chi, H_\theta, \delta)$ results from substituting the QSSE H_θ into Eq.(39), and given by

$$\bar{H}_\gamma(\chi, H_\theta, \delta) = A_1 \pm A_2\sqrt{A_3 + A_4H_\theta + A_5\delta}, \tag{44}$$

where χ is treated as a fixed parameter. The control strategy that will be presented in the following section uses this time-scale separation strategy to obtain a sequential control strategy that permits to stabilize each of the different subsystems (Σ_S, Σ_I, Σ_F and Σ_U).

V. Sequential Singular Perturbation Control Strategy

The control strategy goal consists in designing feedback control laws permits to follow known references in velocity (V_{ref}) and flight path angle (γ_{ref}). Following γ_{ref} is attained by ensuring desired pitch rate, flight path angle and pitch angle dynamics with the use of the elevator deflection (δ), while following V_{ref} is achieved with the throttle position (δ_T). The use of sequential time-scale decomposition permits to design control strategies for δ based on the sum of three components, $\delta = \delta_\theta + \delta_\gamma + \delta_q$, where each component is specifically designed to stabilize each one of the associated boundary layer subsystems, that is, $\delta_q = \Gamma_q(\chi, \theta, \gamma, q)$ for the ultrafast subsystem, Eq. (33), $\delta_\gamma = \Gamma_\gamma(\chi, \theta, \gamma)$ for the fast subsystem, Eq. (38), and $\delta_\theta = \Gamma_\theta(\chi, \theta)$ for the intermediate subsystem, Eq. (42).

In order to guarantee the validity of the sequential control strategy, a series of requirements on the control strategies need to be satisfied. The ultra-fast feedback control δ_q is designed to satisfy two crucial requirements, as seen in [1]: when the ultra-fast feedback function, δ_q, is applied to the boundary layer Eq. (33), the closed-loop system should remain a standard SPS, which translates to that the equilibrium of the boundary layer

$$0 = f_q(\chi, \theta, \gamma, q, \Gamma_\theta + \Gamma_\gamma + \Gamma_q), \tag{45}$$

should have a unique root given by $\bar{q} = H_q(\theta, \gamma, \Gamma_\theta + \Gamma_\gamma)$ in $B_\chi \times B_\theta \times B_\gamma \times B_q$. This requirement assures that the choice of Γ_q will not destroy this property of function f_q in the open-loop system. The second requirement on $\Gamma_q(\chi, \theta, \gamma, q)$ is that it be *inactive* for $\bar{q} = H_q(\theta, \gamma, \Gamma_\theta + \Gamma_\gamma)$, that is

$$\Gamma_q\left[\chi, \theta, \gamma, H_q(\chi, \theta, \gamma, \Gamma_\theta + \Gamma_\gamma)\right] = 0. \tag{46}$$

Similarly, two requirements need to be satisfied by the (fast) control feedback δ_γ such that when applied to the boundary layer Eq. (38), the closed-loop system should remain a standard singularly perturbed system, which translates to that the equilibrium of the boundary layer

$$0 = f_\gamma(\chi, \theta, \gamma, \Gamma_\theta + \Gamma_\gamma), \tag{47}$$

should have a unique root given by $\bar{\gamma} = H_\gamma(\chi, \theta, \Gamma_\theta)$ in $B_\chi \times B_\theta \times B_\gamma$. This requirement assures that the choice of Γ_γ will not destroy this property of function f_γ in the open-loop system. The second requirement in δ_γ, is that it be *inactive* for $\bar{\gamma} = H_\gamma(\chi, \theta, \Gamma_\theta)$, that is

$$\Gamma_\gamma\left[\chi, \theta, H_\gamma(\chi, \theta, \Gamma_\theta)\right] = 0. \tag{48}$$

With this in mind, the control strategy starts by applying the stretched time-scale τ_3 resulting in the reduced order Σ_{SIF}-subsystem, Eqns. (29–32) with the boundary layer Σ_U-subsystem given by Eq. (33), and with the quasi-steady-state equilibrium given by Eq. (34). The reduced order order Σ_{SIF}-subsystem can be decomposed again by applying the stretched time-scale τ_2 resulting in the reduced order Σ_{SI}-subsystem, Eqns. (35–37), and the boundary layer Σ_F-subsystem given by Eq. (38), with the equilibrium $H_\gamma(\chi, \theta, \delta_\theta)$ given by Eq. (39). The Σ_{SI}-subsystem, Eqns. (35–37), can be decomposed again by applying the last stretched time-scale τ_1, resulting in the new reduced order Σ_S-subsystem, Eqns. (40–41), with the boundary layer Σ_I-subsystem given by Eq. (42).

Recall that according to Eqns. (46) and (48), Γ_q and Γ_γ become *innactive* when appearing in their respective equilibria in the Σ_I-subsystem, thus becoming $\delta = \delta_\theta$. The control signal δ_θ is therefore selected as a feedback linearization signal for a target system of the form

$$\frac{\mathrm{d}\theta}{\mathrm{d}\tau_1} = -\tilde{b}_\theta \left(\theta - \theta_{ref}\right), \tag{49}$$

where $\tilde{b}_\theta = \varepsilon_1 b_\theta$, with b_θ being the desired transient response for the Σ_I-subsystem, and θ_{ref} defined in terms of V_{ref} and γ_{ref} by the equilibrium analysis of the problem given by Eqns. (11–15). The control signal is therefore selected as

$$\begin{aligned} \delta_\theta &= B_1 \pm B_2\sqrt{B_3 + B_4\theta + B_5\left(\theta - \theta_{ref}\right)} + B_6\theta \\ &+ B_7\left(\theta - \theta_{ref}\right), \end{aligned} \tag{50}$$

with $B_1 = \bar{a}_{16}^2 A_2^2 A_5/(2\bar{a}_{17}^2) - \bar{a}_{15}/\bar{a}_{17} + \bar{a}_{16}A_1/\bar{a}_{17}$, $B_2 = -\bar{a}_{16}A_2/(2\bar{a}_{17}^2)$, $B_3 = \left(\bar{a}_{16}A_2A_5\right)^2 - 4\bar{a}_{15}a_{17}A_5 + 4\bar{a}_{16}\bar{a}_{17}A_1A_5 + 4\bar{a}_{17}^2A_3$, $B_4 = 4\bar{a}_{17}^2A_4 - 4\bar{a}_{16}\bar{a}_{17}A_5$, $B_5 = 4\bar{a}_{17}\bar{a}_{18}A_5\tilde{b}_\theta$, $B_6 = -\bar{a}_{16}/\bar{a}_{17}$, and $B_7 = \bar{a}_{18}\tilde{b}_\theta/\bar{a}_{17}$, and where it can be shown that that positive solution of Eq. (50) is the right one. With the boundary layer Σ_I-subsystem stabilized and δ_θ defined, the reduced order Σ_S-subsystem can be stabilized by selecting a feedback linearization control signal δ_T such that the velocity dynamics has a desired target dynamics of the form

$$\dot{V} = -b_V\left(V - V_{ref}\right), \tag{51}$$

with b_V being the desired transient response for the Σ_S-subsystem, thus selecting

$$\begin{aligned} \delta_T &= -\frac{1}{a_1 + a_2V^2 + a_3V}\left[\left(a_4 + a_5\right)V^2 + V^2\left[\left(a_6\right.\right.\right. \\ &+ a_7\left(H_\theta - \bar{H}_\gamma\right) + a_{10}\delta_\theta\Big)\left(H_\theta - \bar{H}_\gamma\right) + \left(a_8 + a_9\delta_\theta\right)\delta_\theta\Big] \\ &+ a_{11}\left(\bar{H}_\gamma - \frac{\bar{H}_\gamma^3}{6}\right) + b_V\left(V - V_{ref}\right)\Bigg]. \end{aligned} \tag{52}$$

The Σ_F-subsystem, Eq. (38) is stabilized by selecting the control signal δ_γ, recalling that needs to satisfy Eqns. (47–48). This is achieved by substituting first δ_θ into the Σ_F-subsystem, and rewriting the result in terms of its equilibrium H_γ, Eq. (39), by identifying that the original system is a function of the two possible solutions, that is

$$\frac{\mathrm{d}\gamma}{\mathrm{d}\tau_2} = -\frac{\bar{a}_{11}}{2V}\left[\gamma - H_\gamma(\chi,\theta,\delta_\theta)\right]\left[\gamma - \tilde{H}_\gamma(\chi,\theta,\delta_\theta)\right] + V\bar{a}_{14}\delta_\gamma, \tag{53}$$

Note also that according to Eq. (46), Γ_q becomes *innactive* when appearing in its equilibrium in the Σ_F-subsystem, thus, $\delta = \delta_\theta + \delta_\gamma$, with δ_θ being given by the control signal that stabilizes the Σ_I-subsystem, Eq. (50). Note that $H_\gamma(\chi,\theta,\delta_\theta)$ represents the positive solution of Eq. (39), while $\tilde{H}_\gamma(\chi,\theta,\delta_\theta)$ represents the disregarded negative solution, but both being necessary to complete the solution. The control signal δ_γ it is selected as a feedback linearization control signal for a selected target system of the form

$$\frac{\mathrm{d}\gamma}{\mathrm{d}\tau_2} = -\tilde{b}_\gamma\left[\gamma - H_\gamma(\chi,\theta,\delta_\theta)\right], \tag{54}$$

where $\tilde{b}_\gamma = \varepsilon_1\varepsilon_2 b_\gamma$, with b_γ being the desired transient response for the Σ_F-subsystem. The choice of this target dynamics will satisfy that the choice of Γ_γ will not destroy the property that the closed-loop system should have a unique equilibrium $\bar{\gamma} = H_\gamma(\chi,\theta,\Gamma_\gamma)$, and that Γ_γ it be *inactive* for $\bar{\gamma} = H_\gamma(\chi,\theta)$, resulting in

$$\delta_\gamma = \frac{\left(\gamma - H_\gamma\right)\left[-\tilde{b}_\gamma + \frac{\bar{a}_{11}}{2V}\left(\gamma - \tilde{H}_\gamma\right)\right]}{\bar{a}_{14}V}. \tag{55}$$

With control signal δ_γ selected, the control signal δ_q that stabilizes the Σ_U-subsystem can be selected by ensuring requirements (45-46). Recall that for the Σ_U-subsystem, $\delta = \delta_\theta + \delta_\gamma + \delta_q$, therefore, by substituting δ_θ and δ_γ, Eqns. (50) and (55), respectively, into the Σ_U-subsystem, and rewriting it using the definition of the H_q QSSE, Eq. (34), results in

$$\frac{\mathrm{d}q}{\mathrm{d}\tau_3} = V^2\left[\bar{a}_{18}\left[q - H_q(\chi,\theta,\gamma,\delta_\theta + \delta_\gamma)\right] + \bar{a}_{17}\delta_q\right]. \tag{56}$$

Similarly, in order to satisfy Eqns. (45-46) on the control signal δ_q, lets choose a feedback linearization control signal for a selected target system of the form

$$\frac{\mathrm{d}q}{\mathrm{d}\tau_3} = -\tilde{b}_q\left[q - H_q(\chi,\theta,\gamma,\delta_\theta + \delta_\gamma)\right], \tag{57}$$

where $\tilde{b}_q = \varepsilon_1\varepsilon_2\varepsilon_3 b_q$, with b_q being the desired transient response for the Σ_U-subsystem, resulting in

$$\delta_q = -\frac{\left(\tilde{b}_q + \bar{a}_{18}V^2\right)\left[q - H_q(\chi,\theta,\gamma,\delta_\theta + \delta_\gamma)\right]}{V^2\bar{a}_{17}}. \tag{58}$$

This finalizes the control strategy with the control signals given by $\delta = \delta_\theta + \delta_\gamma + \delta_q$, Eqns. (50), (55), and (58), respectively, and δ_T, Eq. (52). Following section provides some simulation results.

VI. Numerical Results

This section presents some results corresponding to the simulations conducted to analyze the proposed control law. The numerical simulation uses a fourth-order Runge-Kutta fixed step integration method, with a time step of 0.001 seconds, written in the $MATLAB$ interface. The analysis includes variation in the references V_{ref} and γ_{ref}. Actuator saturations are also included, namely $-40^\circ \leq \delta \leq 40^\circ$, and $0 \leq \delta_T \leq 1$.

Different cases will be considered: varying V_{ref}, while maintaining $\gamma_{ref} = 0$; varying γ_{ref}, while maintaining $V_{ref} = const$; and varying both γ_{ref} and V_{ref}. Results for this last case are presented in Fig. 1 and 2, where constant acceleration and deceleration references are also generated, with 30 seconds per maneuver. Figure 1 shows the states: the altitude and aerodynamic airspeed, on the top row, pitch and flight path angle on the middle row, angle of attack and pitch rate on the bottom row; and Fig. 2 shows the control: elevator deflection and throttle position. The different variable reference set points are presented with a thinner red line. Note that it is also included a reference in altitude given by $h_{ref} = V_{ref}\sin\gamma_{ref}$, despite that the control strategy is focused on following both by separate, but serves to indicate that future control strategies will be derived so follow altitude profiles. Despite the complex reference profiles, the control strategy is able to follow them in both aerodynamic velocity and flight path angle. Also note that saturations are avoided by selecting the appropriate desired dynamic coefficients, $b_V = b_\theta = b_\gamma = b_q = 0.35$.

VII. Conclusions

The presented control strategy permits to drive the UAV to follow variable references in both aerodynamic velocity and flight path angle by using a sequential strategy that permits to easily obtain appropriate feedback control laws that stabilize each of the subsystems. The control strategy provides a closed-form solution. The simulations were conducted using a realistic model of the Cefiro aircraft developed by the Dept. of Aerospace Engineering at the University of Seville [14], which will the platform where the future flight tests and validation of the control strategies will be conducted.

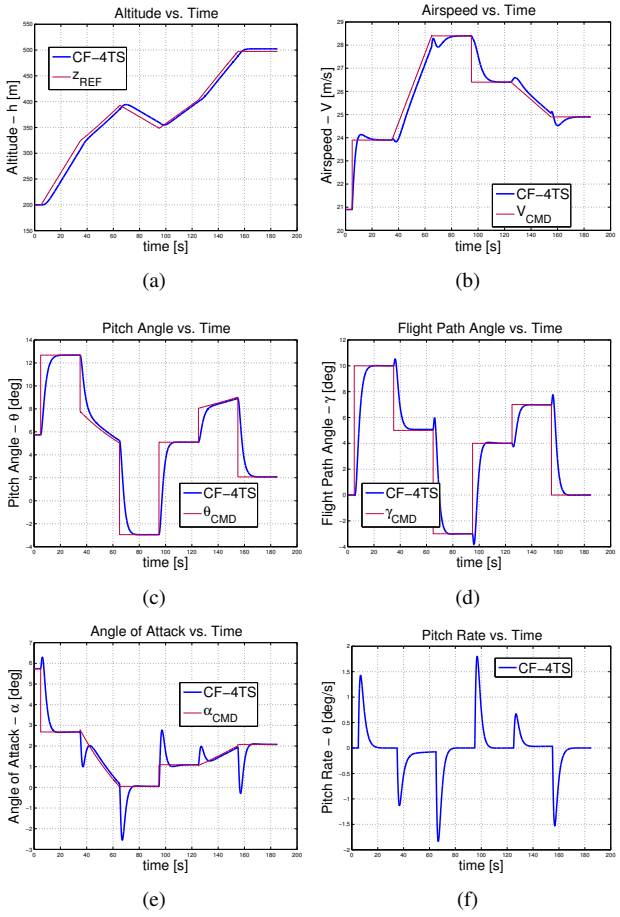

Fig. 1. State history for simulations with variable V and γ.

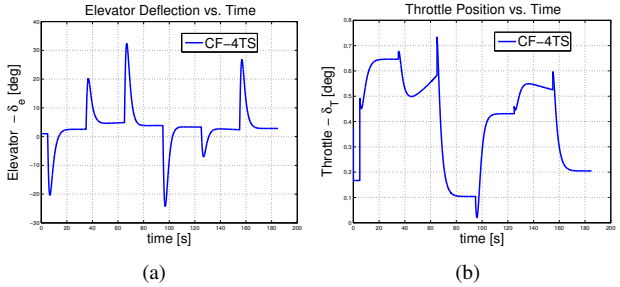

Fig. 2. Control history for simulations with variable V and γ.

References

[1] P. Kokotović, H. Khalil, and J. O'reilly, *Singular perturbation methods in control: analysis and design*. Society for Industrial Mathematics, 1999, pp. 189–320.

[2] S. Esteban, F. Gordillo, and J. Aracil, "Three-Time Scale Singular Perturbation Control and Stability Analysis for an Autonomous Helicopter on a Platform," *International Journal of Robust and Nonlinear Control*, pp. 1–34, 2012, accepted for publication 11 March 2012.

[3] R. Brockett, "Feedback invariants for nonlinear systems," in *A link between science and applications of automatic control: proceedings of the seventh Triennial World Congress of the IFAC, Helsinki, Finland*. IFAC, June 1978, pp. 1115–1120.

[4] J. Buffington, A. Sparks, and S. Banda, "Full conventional envelope longitudinal axis flight control with thrust vectoring," in *American Control Conference*. IEEE, 1993, pp. 415–419.

[5] H. Sira-Ramírez, M. Zribi, and S. Ahmad, "Dynamical Sliding Mode Control Approach for Vertical Flight Regulation in Helicopters," *IEE Proceedings-Control Theory & Applications*, vol. 141, no. 1, pp. 19–24, 1994.

[6] H. Khalil, *Nonlinear Systems*. Prentice Hall, 1996.

[7] F. Gavilan, J. Acosta, and R. Vazquez, "Control of the longitudinal flight dynamics of an uav using adaptive backstepping," in *IFAC World Congress, Milan, Italy*, 2011.

[8] S. Balakrishnan and V. Biega, "Adaptive-critic-based neural networks for aircraft optimal control," *Journal of Guidance, Control, and Dynamics*, vol. 19, no. 4, pp. 893–898, 1996.

[9] S. Balakrishnan and S. Esteban, "Nonlinear flight control systems with neural networks," in *Proceedings of the AIAA Guidance, Navigation and Control Conference and Exhibit, Montreal*. AIAA, August 2001.

[10] D. Naidu and A. Calise, "Singular perturbations and time scales in guidance and control of aerospace systems: A survey," *Journal of Guidance, Control and Dynamics*, vol. 24, no. 6, pp. 1057–1078, 2001.

[11] R. Mehra, R. Washburn, S. Sajan, and J. Carrol, "A study of the application of singular perturbation theory," NASA CR-3167, 1979.

[12] S. Bertrand, N. Guénard, T. Hamel, H. Piet-Lahanier, and L. Eck, "A hierarchical controller for miniature vtol uavs: Design and stability analysis using singular perturbation theory," *Control Engineering Practice*, 2011.

[13] S. Esteban, "Three-time-scale Control of an Autonomous Helicopter on Platform," Automatics, Robotics and Telematic Ph.D., Universidad de Sevilla, Sevilla, Spain, July 2011.

[14] C. Bernal, A. Fernandez, P. Lopez, A. Martin, D. Perez, F. Samblas, S. Esteban, F. Gavilan, and D. Rivas, "Cefiro: an aircraft design project in the university of seville," in *9th European Workshop on Aircraft Design Education (EWADE 2009)*, 2009.

[15] B. Etkin and L. Reid, "Dynamics of flight: stability and control."

[16] J. Roskam, *Airplane flight dynamics and automatic flight controls*. DARcorporation, 2001.

[17] A. Calise, "A singular perturbation analysis of optimal thrust control with proportional navigation guidance," in *IEEE Conference on Decision and Control*. IEEE, 1977, pp. 1167–1176.

[18] ——, "Optimization of aircraft altitude and flight-path angle dynamics," *Journal of Guidance, Control, and Dynamics(ISSN 0731-5090)*, vol. 7, pp. 123–125, 1984.

[19] M. Ardema and N. Rajan, "Separation of Time-Scales in Aircraft Trajectory Optimization," *Journal of Guidance, Control, and Dynamics*, vol. 8, no. 2, pp. 275–278, 1985.

[20] ——, "Slow and fast state variables for three-dimensional flight dynamics," *Journal of Guidance, Control, and Dynamics*, vol. 8, no. 4, pp. 532–535, 1985.

[21] M. Heiges, P. Menon, and D. Schrager, "Synthesis of a helicopter full-authority controller," *Journal of Guidance, Control, and Dynamics*, vol. 15, no. 1, pp. 222–227, 1992.

[22] B. Sridhar and N. Gupta, "Missile guidance laws based on singular perturbation methodology," *Journal of Guidance and Control*, vol. 3, pp. 158–165, 1980.